

An analytical study of blasting vibration using deep mining and drivage rules

Xianglong Li^{1,2} · Hui Hu¹ · Lihua He³ · Kegang Li¹

Received: 8 October 2016 / Revised: 28 December 2016 / Accepted: 4 January 2017 / Published online: 10 January 2017
© Springer Science+Business Media New York 2017

Abstract For the study on the propagation–attenuation rule of the blasting vibration wave in the deep mining roadway of Shizishan copper mine, and the analysis of the influences of different maximum explosive charges and different underground systems on the propagation of blasting vibration signals, blasting vibration monitoring of the two different situations has been carried out respectively. Firstly, the Sadov’s Formula has been applied to analyzing the monitoring results of the mining roadway, and thus the value of its excavation blasting vibration attenuation index K and α and its corresponding regression formula were attained; then, the appropriate regression formula was used to calculate the maximum explosive charge which could ensure the safety of the principal chambers underground the mine. Meanwhile, on the basis of the HHT analysis method, the rule of vibration wave propagation under these two different situations was analyzed. And the results indicated that, whether with an increase in the single charge, or with an increase in the number of the underground systems to cross, blasting seismic wave had a tendency for spreading to the low-frequency band. Through the regression analysis of the Sadov’s Formula and the HHT Method, the results provided a reliable basis for the safe and efficient production of the mine.

Keywords Deep mining · Blasting vibration · Sadov’s formula · HHT · Propagation law

✉ Xianglong Li
xianglongmail@126.com

¹ Faculty of Land Resource Engineering, Kunming University of Science and Technology, Kunming 650093, Yunnan, China

² State Key Laboratory of Explosion Science and Technology, Beijing Institute of Technology, Beijing 100081, China

³ Faculty of Mining Industry, Kunming Metallurgy College, Kunming 650033, China

1 Introduction

Blasting seismic waves are the inevitable products of explosive detonation. Although only a small part of the energy released from the explosive detonation is converted into the energy of seismic waves, if not controlled properly, it will also harm the surrounding environment of the explosion area and may cause huge casualties and economic losses. Only by analyzing and studying the type and the propagation regulation of blasting seismic waves can we further study the damage mechanism of blasting vibration more effectively, making the blasting vibration disaster effectively controlled, and thus protecting the safety of structure [1, 2]. Monitoring of blasting vibration aims at having a better understanding and mastery of characteristics of blasting seismic wave, its propagation rule and the mechanism how it causes influence and damage to buildings (structures) so as to prevent and reduce damage caused by blasting vibration to structures and reduce the harm brought about by blasting seismic wave to the greatest extent [3–5].

Nowadays, main research work of experts and scholars focuses on influence of seismic effect caused by surface blasting on surrounding and near buildings, influence of blasting vibration effect caused by tunnel drivage on adjacent tunnel and surrounding rocks around the tunnel [6–9], influence of open-pit mine blasting vibration on high and steep slope stability, blasting seismic wave propagation and attenuation rules and energy distribution features under different geological and construction conditions [10–18], etc. However, there are few researches on blasting vibration effect in metal mine underground mining and its influence on surrounding rock, tunnel and special chamber, they are basically of no systematicness, so there is a lot remained to be perfected.

This paper monitored blasting vibration during production blasting of Shizishan copper mine, studied propagation

Table 1 Crustal stress calculation results summary table

Measuring point	The maximum main stress			The intermediate principal stress			The minimum principal stress		
	Numerical value (MPa)	Direction (°)	Angle (°)	Numerical value (MPa)	Direction (°)	Angle (°)	Numerical value (MPa)	Direction (°)	Angle (°)
9th level	19.70	135.45	0.27	14.89	44.91	63.25	9.87	225.58	26.75
11th level	12.69	269.39	−11.37	9.61	−4.36	18.05	7.66	210.00	68.46
12th level	39.41	245.75	3.17	34.59	−14.97	71.07	20.87	154.68	18.65
15th level	37.7	163.72	6.97	14.48	75.62	−15.14	13.05	229.73	−73.26

and attenuation rules of blasting seismic wave and blasting energy in the deep underground high in-situ stress stope as well as influence of maximum single blow blasting charge and number of spanned underground systems on propagation rule of blasting seismic waves, thus controlling the scale of blasting operation and explosion energy, providing basis for prevention against blasting hazard in order to ensure the safety and orderly production of the mine.

2 Engineering geology

The mine lot is located on Yunnan-Guizhou Plateau, east bank of Lvzhi River, northwestern part of Yimen Dam and it belongs to middle mountain landform. Shizishan copper mine mineral deposit is under control of a series of sharply plunging and closely inversed folds, and its axial direction is N45°–62°E. Anticline core stratum consists of sodium silica rock in Xinzhuang, and stratums at both wings are respectively silica dolomite in Pingyang and brown silica slate in Guoshuigou.

At present, production engineering in Shizishan copper mine mainly includes 15th level of phase III project and phase IV project in Shizishan copper mine. The 16th level in phase IV project is the main mining level, and the 17th and 18th levels are at started drivage stage; main production area is located at “Xipiao” ore belt in the 15th and 16th levels. Ore body in this study is the one located at “Xipiao” ore belt in the 16th level, and it belongs to deep mining ore body.

Divided by the absolute size of the ground stress, the maximum stress of the rock mass is considered to be in the high ground stress state when the maximum principal stress reaches 20–30 MPa. Combined with the ground stress test results of the middle section in the following table, we can conclude that: the ground stress of the deep part of Shizishan copper mine belongs to high ground stress.

The results of partial levels stress calculation are shown in Table 1 [19].

The height of phase 4 of the project is generally 50 m, the average thickness of the ore body is about 25 m, strike N45°–55°E, dip angle 65°–85°, inclination ES, and the average

length of strike is 360m. The rock solid coefficient is $f=6-8$, belonging to the solid rock. The 16th level consists of main ore body, slate ore body, ribbon ore body and No. 4 ore body, ore bodies are stored in cinerous and hoary dolomite stratum and stratum purple slate mingled with dolomite. At heading side of surrounding rock of ore body are cinerous dolomite, purple slate mingled with dolomite and purple slate in Yinmin formation, and at handing side are hoary dolomite and purple slate.

The macro physical and mechanical parameters of rock mass in oreas shown in Table 2 [19].

3 Blasting vibration monitoring method

3.1 Monitoring physical quantity

In project, the physical quantity with the highest destructive power to protected objects is generally chosen as the main monitoring object. In actual monitoring of blasting vibration, the monitoring of the peak velocity and peak acceleration of blasting vibration is the most extensive. At present, according to the requirements of Safety Regulations for Blasting (GB6722-2014) [20], the blasting vibration velocity and the strength of the corresponding vibration frequency are considered as the main measurement criteria to determine whether it produces damage to the protected objects. From mechanics point of view, the particle vibration in blasting vibration can be simplified to simple harmonic vibration, and the relationship between ultimate stress and maximum vibration velocity, elastic modulus and wave propagation velocity in the medium of the structure is as Eq. 3.1 [21].

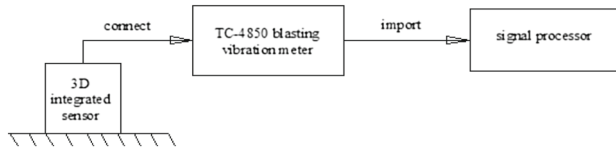
$$\alpha_m = \frac{V_m E}{c} \quad (3.1)$$

where α_m —Max. stress that the structure can bear; E —elastic modulus of the structure; c —propagation velocity of the vibration wave in the structure; V_m —max. vibration velocity of particle in the structure.

From Eq. 3.1, it can be seen that with the increase of blasting vibration velocity, the stress of the structure will increase,

Table 2 Table of mechanical properties of macro rock mass in Shizishan Copper Mine

Lithology	Average volume weight (g/cm ³)	Tensile strength (MPa)	Elastic modulus (×10 ⁴ MPa)	Poisson ratio	Group cohesiveness <i>c</i> /(MPa)	The angle of internal friction ϕ (°)
Cineros dolomite	2.83	2.956	20.01	0.269	2.611	41.99
Hoary dolomite	2.76	2.796	13.06	0.280	2.550	34.05
Purple slate	2.63	4.52	4.34	0.284	1.571	31.68

**Fig. 1** Schematic diagram of blasting vibration testing system

so the blasting vibration velocity can be used to judge whether the blasting vibration will destroy the structure. But in blasting vibration, the vibration velocity of slope rock particle is divided into three directions: radial, tangential and vertical. While the destruction of the slope is mainly shear failure, from Eqs. 3.2 of rock shear strength, we can conclude that [22] :

$$\tau = C + \sigma \tan \beta \quad (3.2)$$

where τ —shear strength, β —internal friction angle, σ —normal stress, C —cohesive force.

The cohesion and internal friction angle of the rock are generally constant, so the shear strength decreases as the normal stress of the rock decreases. In the vibration velocity of blasting vibration in three directions, the vertical vibration will have a greater impact on the normal stress of slope rock mass. When the vertical velocity of particle vibration is greater, the normal stress of the slope rock will reduce, and the shear strength of the rock will also reduce, when the slope is prone to instability. Therefore, in the blasting vibration velocity monitoring, this paper mainly takes the vibration velocity of vibration wave in the vertical direction and its corresponding frequency as the studied object.

3.2 Monitoring system and method

This blasting monitoring system consisted of TC-4850 blasting vibration meter and its matched 3D integrated sensor and signal processor produced by Chengdu Zhongke Measurement and Control Co., Ltd, as shown in Fig. 1

As propagation distance increased, vibration effect of blasting is gradually weakened, hence, generally the sensor was fixed at the position nearby blasting source, in the meantime, X axis of sensor pointed to blasting source, and Z axis

pointed to vertical direction. Blasting vibration meter would automatically acquire and store data during blasting process.

4 Field vibration monitoring

4.1 Monitoring point arrangement

In order to explored into propagation and attenuation rules of blasting energy and blasting seismic wave, studied influence of maximum single blow blasting charge on blasting seismic wave signals as well as influence of underground roadway of mine on propagation rule of blasting seismic waves and predicted blasting vibration strength, thus providing basis for prevention against blasting hazard, control of explosion energy, control of large blasting scale and determination of vibration standard for large blasting construction. Blasting vibration signal monitoring was implemented on blasting production in “Xipiao” ore belt in the 16th middle section of main mining area of the mine. For different research orientations, monitoring points arranged in data collection were also different (whereby monitoring point arrangements in vibration monitoring on December 4th and December 11th were as shown in Figs. 2, 3).

4.2 Monitoring results

After several days of testing, obtained the signal data as shown in Tables 3 and 4 respectively at the same level and different levels.

5 Processing and analysis of monitoring data

5.1 Regression analysis of blasting vibration velocity and setting of maximum single blow blasting charge

5.1.1 Regression analysis of blasting vibration velocity

According to permissible standard about blasting vibration safety as stipulated in Safety Regulations for Blasting (GB6722-2014) [20], only from dominant frequency and velocity of peak vibration velocity in vertical direction, influ-

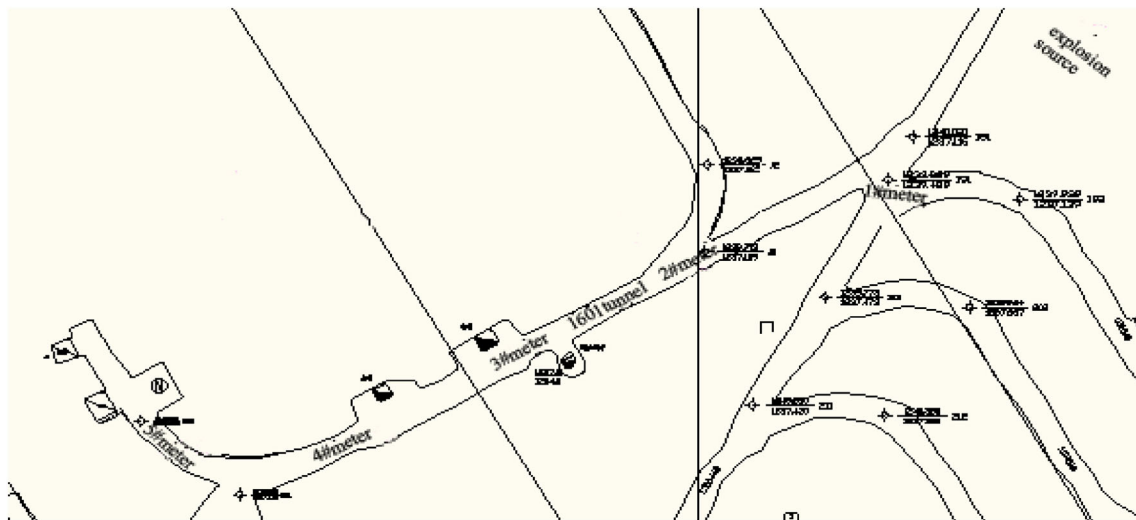
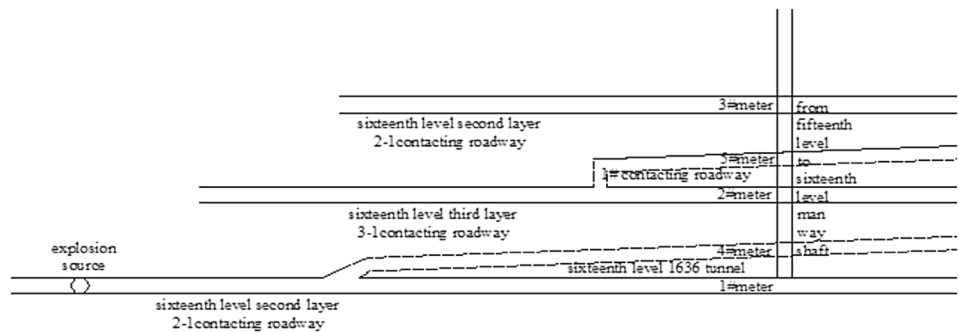


Fig. 2 On December 4th the same level of vibration monitoring point layout diagram

Fig. 3 On December 11th the different levels of vibration monitoring point layout diagram



ence of each production blasting operation on surrounding buildings must be within national standard range. There are many factors which can influence attenuation rule of mass point blasting vibration, including exploding conditions (blast hole diameter and depth of blasting source, charging constitution, etc.) and local geological site conditions (rock mass conditions, site conditions, relative positional relationship with blasting source, etc). In current engineering application, most use Sadoy’s empirical formula [20–23] to analyze relationship between mass point vibration velocity and charging amount and blasting center distance:

$$V = K \left(Q^{1/3} / R \right)^\alpha \tag{5.1}$$

In the formula: V —maximum blasting vibration velocity of mass point (cm/s); Q —explosive charge, simultaneous blasting was total explosive charge, and postponed blasting was maximum single blow blasting charge, (kg); R —distance from blasting source to monitoring point (m); both K and α were coefficient and attenuation index related to landform and geological conditions from blasting point to monitoring point.

According to blasting vibration test results, we respectively conducted regression analysis of monitoring data which tool different maximum single blow blasting charges and different underground mining systems as main influencing factors and then used MATLAB software to do regression of Sadoy’s formula, and regression results were as shown in Figs. 4, 5, and 6.

After linear regression was implemented on collected data, it is necessary to transform the formula into linear equation and then conduct regressive calculation. We simultaneously took logs base e at both sides of Eq. (3.1), then: $\ln V = \ln K + \ln(Q^{1/3}/R) \cdot \alpha$.

We set $y = \ln V, a = \ln K, b = \alpha, x = \ln K + \ln(Q^{1/3}/R)$, namely transforming the formula into standard linear equation:

$$y = b \cdot x + a \tag{5.2}$$

According to transformation criterion, a comparison between equations in standard equation and linear regression chart was made, then values of K and α of coefficient and attenuation index related to landform and geological conditions from

Table 3 The same level of the blasting vibration signal data

Date	Blasting area	N	G (kg)	L (m)		Channel X		Channel Y		Channel Z	
						V (cm/s)	f (Hz)	V (cm/s)	f (Hz)	V (cm/s)	f (Hz)
11-24	16th level	1#	3	85	0.0489	554.234	0.0516	456.328	0.0572	654.254	
		2#		138	0.0435	565.254	0.0218	518.365	0.0311	647.364	
		3#		179	0.0208	627.658	0.0218	625.658	0.0215	567.253	
		4#		208	0.0168	556.256	0.0158	465.226	0.0182	526.665	
		5#		240	0.0098	610.596	0.0103	524.596	0.0144	452.354	
11-30		1#	3	60	0.0449	533.357	0.0613	307.681	0.0897	666.644	
		2#		135	0.0254	645.681	0.0384	446.581	0.0315	646.581	
		3#		180	0.0203	613.547	0.0548	635.157	0.0212	563.147	
		4#		225	0.0156	565.308	0.0128	563.218	0.0159	515.258	
		5#		268	0.0112	435.054	0.0103	624.653	0.0136	425.064	
12-4		1#	9	80	0.0702	382.355	0.0685	383.285	0.0974	685.325	
		2#		140	0.0448	445.318	0.0625	465.378	0.0485	654.328	
		3#		180	0.0394	376.234	0.0389	279.243	0.0331	589.234	
		4#		210	0.0238	467.342	0.0205	434.382	0.0291	483.352	
		5#		240	0.0196	386.524	0.0165	345.254	0.0240	389.254	
12-9		1#	9	60	0.1044	470.424	0.1609	433.355	0.1402	445.420	
		2#		110	0.0592	450.659	0.0896	382.435	0.0673	432.254	
		3#		180	0.0389	429.325	0.0584	421.325	0.0322	428.328	
		4#		215	0.0198	368.354	0.0225	463.285	0.0235	405.365	
		5#		255	0.0156	369.485	0.0172	396.548	0.0213	368.459	

Table 4 The different levels of the blasting vibration signal data

Date	Blasting area	N	G (kg)	L (m)		Channel X		Channel Y		Channel Z	
				l	h	V (cm/s)	F (Hz)	V (cm/s)	f (Hz)	V (cm/s)	f (Hz)
12-11	16th level	1#	12	165	0	0.0247	153.480	0.0212	242.445	0.0393	156.879
		2#		165	10	0.0252	148.965	0.0215	248.624	0.0368	146.251
		3#		165	20	0.0204	138.383	0.0206	256.234	0.0342	135.265
		4#		165	0	0.0235	153.360	0.0216	242.355	0.0389	158.579
		5#		165	10	0.0216	147.456	0.0213	213.589	0.0365	143.321
12-14		1#	12	120	0	0.0191	363.647	0.0424	285.726	0.0676	287.264
		2#		120	10	0.0386	285.120	0.0461	277.702	0.0611	277.777
		3#		120	20	0.0338	215.364	0.0490	235.125	0.0587	234.158
		4#		120	0	0.0193	366.347	0.0415	283.256	0.0673	279.354
		5#		120	20	0.0335	213.598	0.0490	256.218	0.0581	234.052
12-18		1#	12	210	0	0.0202	203.326	0.0401	188.246	0.0302	137.356
		2#		210	10	0.0231	195.235	0.0389	168.327	0.0285	122.258
		3#		210	20	0.0198	201.359	0.0218	143.198	0.0246	110.354
		4#		210	10	0.0215	198.320	0.0365	167.327	0.0285	121.573
		5#		240	20	0.0203	205.361	0.0221	143.128	0.0244	115.384

N instrument serial number, *G* maximum tolerant explosive quantity of single shot, *L* distance from the explosion center, *V* peak vibration velocity, *f* peak vibration frequency, *l* horizontal distance, *h* vertical distance

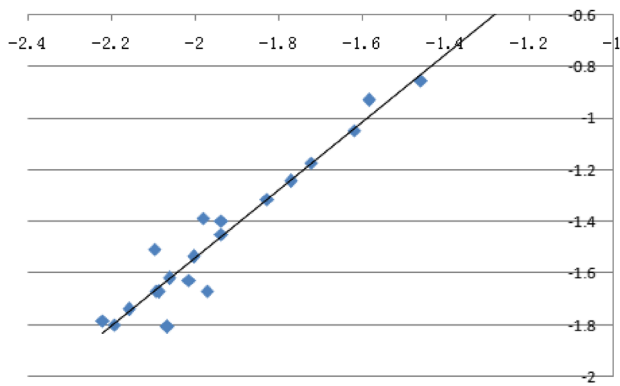


Fig. 4 Linear regression figure of the same level of Sadov’s formula

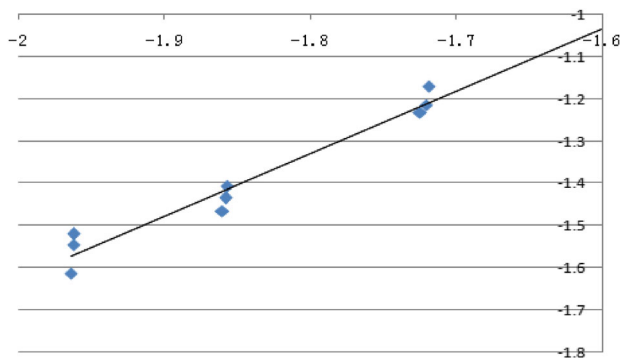


Fig. 5 Linear regression figure of Sadov’s formula under different hierarchies

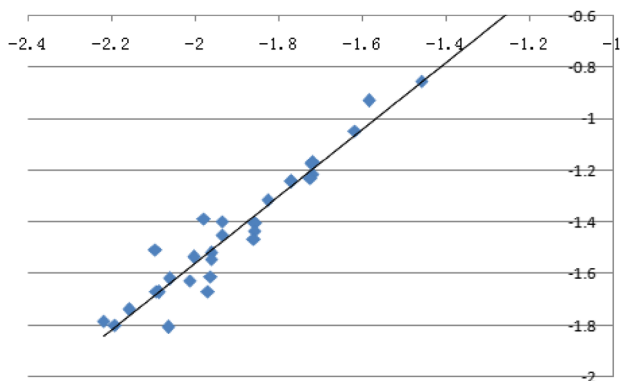


Fig. 6 Linear regression figure of Sadov’s formula in “Xipiao” ore belt in the 16th level

blasting point to monitoring point according to assumptions were calculated.

Linear regression formula of the same level of Sadov’s formula was:

$$V = 380.8 \left(\frac{\sqrt[3]{Q}}{R} \right)^{1.681} \tag{5.3}$$

Linear regression formula of Sadov’s formula under different hierarchies was:

$$V = 281.2 \left(\frac{\sqrt[3]{Q}}{R} \right)^{1.535} \tag{5.4}$$

Linear regression formula of Sadov’s formula in “Xipiao” ore belt in the 16th level was:

$$V = 297.7 \left(\frac{\sqrt[3]{Q}}{R} \right)^{1.615} \tag{5.5}$$

5.1.2 Setting of maximum single blow blasting charge

When blasting area was far away from underground protective chamber and working production area of the mine, blasting vibration had little influence, but with continuous mining of the stope, blasting area would gradually be close to protective chamber and main underground system and mass point vibration velocity would also increase, when mass point vibration velocity of protective chamber or main underground system reached lower limit of mass point vibration velocity stipulated in Safety Regulations for Blasting Practices, setting maximum single blow charge at the moment as that in blasting of “Xipiao” ore belt in the 16th segment was appropriate. It could be known from permissible standard for blasting vibration safety in Safety Regulations for Blasting (GB6722-2014) [20] that: minimum permissible mass point vibration velocity for mine roadway safety was 15 cm/s, we took maximum vibration velocity of vertical component of blasting vibration on the site as 15 cm/s and combined Sadov’s linear regression Eqs. 5.3, 5.4 and 5.5 obtained through fitting to limit maximum single blow blasting charge and conduct maximum blasting charge control at different distances in “Xipiao” ore belt in the 16th level as shown in Table 5.

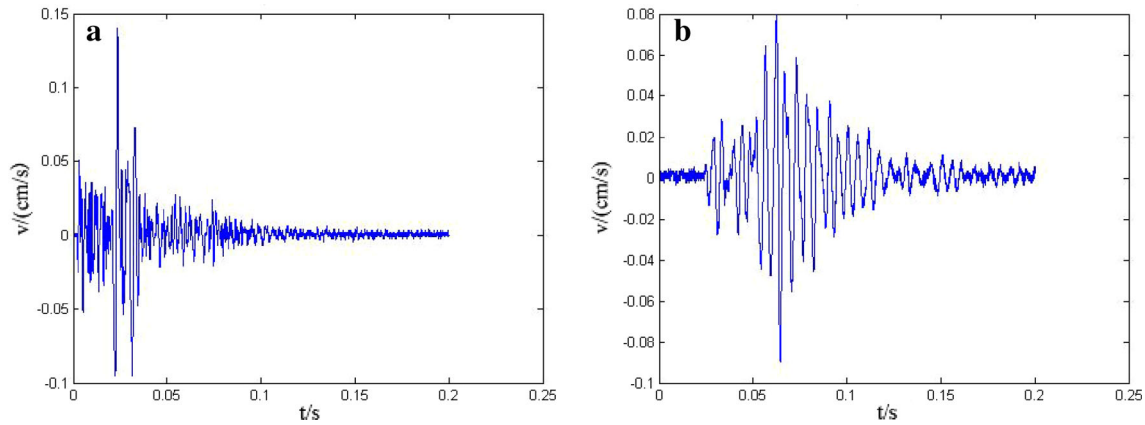
Maximum single blow blasting charge which could safely detonate at different distances from protective chamber could be known from Table 5, in consideration of safety production factors, potential safety hazard should be controlled to the minimum level, and results obtained from-calculation according to Eq. 5.4 were selected to guide on-site actual production blasting.

5.2 Analysis of blasting vibration propagation rule based on HHT algorithm

In order to make more sufficient analysis of measured vibration signals, this time we used HHT [24,25] algorithm to conduct time-frequency analysis of waveform. The Hilbert–Huang transform (HHT) is one of the recognized latest time-frequency local analysis methods built based on the priori wavelet base function and Fourier transform. Its main innovation lies in the proposal of intrinsic mode functions (IMF) and introduction of empirical mode decomposition (EMD). First, a random signal is decomposed into several IMF com-

Table 5 The safety firing table of maximum tolerant explosive quantity of single shot

Distance from the explosion center (m)	20	40	60	80	100	120	140	160
Calculated value for Eq. (5.3)	25	159	470	987	1606	2656	3825	5349
Calculated value for Eq. (5.4)	22	145	381	916	1554	2543	3605	5028
Calculated value for Eq. (5.5)	23	149	406	943	1571	2584	3686	5173

**Fig. 7** Original oscillogram

ponents by EMD method, then the Hilbert transform (HT) is applied to each IMF component to obtain the meaningful instantaneous frequency, so as to meaningful instantaneous frequency [26–31]. The signal can eventually be expressed as the energy distribution on the time-frequency plane, which is called the Hilbert spectrum. The Hilbert Transform mainly reflects the localized characteristics of the signal.

HHT algorithm is one of the recognized latest local time-frequency analysis methods established on basis of Fourier transform on basis of a priori wavelet basis function and wavelet basis function. Hilbert spectrum obtained through this algorithm could describe unstable signals in combined domain of time domain and frequency domain with extremely high time-frequency resolution, and IMF component obtained through EMD transformation was of definite physical significance. HHT algorithm could analyze nonlinear and unstable signals and was of complete adaptivity.

The Hilbert energy spectrum, marginal spectrum and 3D spectrum of the original waveforms measured at various measuring points of the on-site blasting monitoring were obtained through HHT analysis and then processed and analyzed according to different factors of the site to reach the corresponding conclusions.

5.3 Influence of maximum single blow blasting charge on blasting seismic wave

It could be seen from analyses in Tables 2 and 3 that: when maximum tolerant explosive quantity of single shot increased, principal vibration frequency band had tendency

of developing towards low frequency while blasting vibration increased as charge increased.

HHT analysis was made on data collected in Table 2 on MATLAB software. Limited by length, this paper only conducted a comparative analysis of blasting vibration waves collected at monitoring point which was 60m away from blasting source in maximum tolerant explosive quantity of single shot 3 kg (test data of 1# tester on November 30) and maximum tolerant explosive quantity of single shot 9 kg (test data of 1#meter on December 9) as shown in the following figure, Fig. 7a was analysis chart of maximum tolerant explosive quantity of single shot 3 kg, Fig. 7b was analysis chart of maximum tolerant explosive quantity of single shot 9 kg, and original oscillogram after transformation was as shown in Fig. 7.

Figure 8 was energy distribution diagram of blasting vibration signals: energy distribution frequency bands of vibration signals in a mainly concentrated at 40–150 and 0–30Hz, occupancies above 30–40 and 150Hz were small; energy distribution of vibration signals was quite extensive within range of 0–150Hz, and occupancy above 150Hz was also little. However, it could be seen through comparison that energy occupancy of 0–40Hz frequency band in b obviously increased, especially at 2Hz, it occupied about 7.3% in the total energy. This indicated that as single blow blasting charge increased, concentrated frequency band of energy distribution of blasting vibration signals more and more tended to develop towards low frequency band. Figure 9 was about marginal spectrum of blasting vibration signals. It represented all accumulated amplitude in statistical significance and expressed global amplitude of each frequency. It could

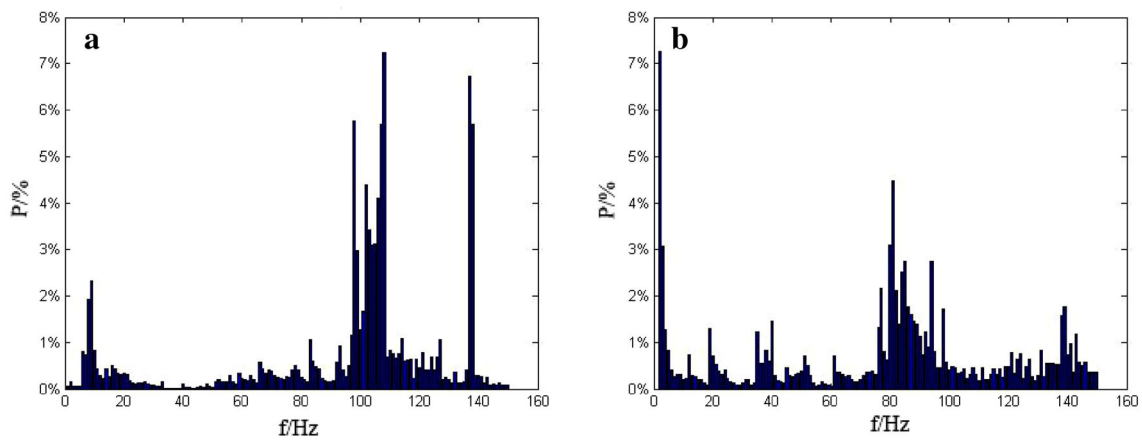


Fig. 8 Energy distribution

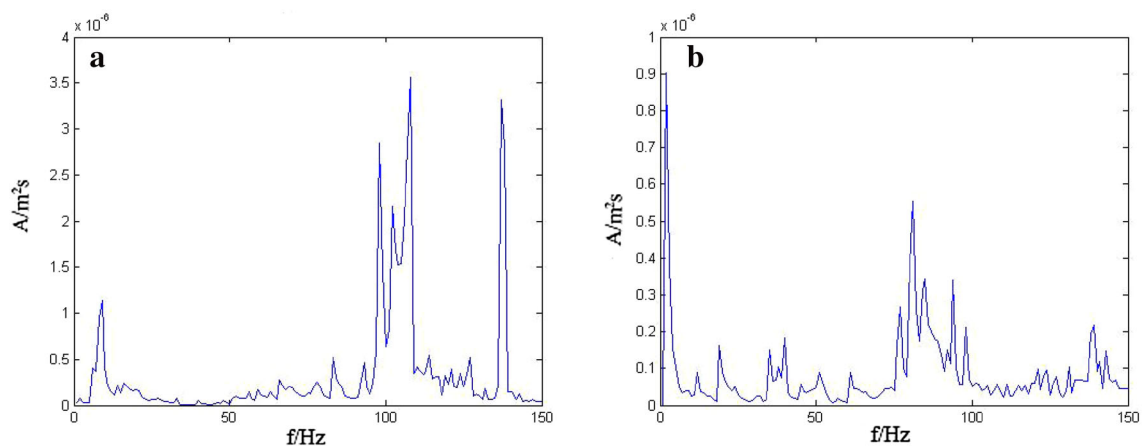


Fig. 9 Marginal spectrum

be seen from a that vibration amplitude within 40–150 Hz was large, and amplitude at 106 Hz reached maximum value; vibration amplitudes within 0–150 Hz frequency band in b were large, while maximum amplitude reached at 2 Hz. This coincided with concentrated energy distribution at this frequency band as analyzed above very well. Figure 10 was 3D spectrum of blasting vibration signals, and its three coordinate axes respectively represented time, frequency and energy of signals. It could be more intuitively seen that energy distribution of vibration signals with time and frequency. In the figure, color code was used to express energy, the higher the energy, the redder the color on color code diagram.

Through a comparative analysis of Figs. 8, 9 and 10, it could be seen that as maximum tolerant explosive quantity of single shot increased, frequency with concentrated energy distribution also lowered, and energy occupancy in low frequency band increased. Natural vibration frequencies of buildings (structures), chamber and tunnel of the mine were also quite low. Hence, energy distribution concentrating on high frequency band was good for protecting safety and stability of all kinds of aboveground and underground

buildings (structures). When major blasting was conducted in deep stope, maximum tolerant explosive quantity of single shot was controlled to make energy of blasting vibration signals distribute at high frequency band, and it is quite necessary to reduce proximity between blasting seismic frequency and natural vibration frequency of buildings (structures).

5.3.1 Influence of underground system on propagation of blasting seismic waves

Under the same maximum tolerant explosive quantity of single shot, monitoring points (data tested by 1#, 2# and 3# testers on December 14) at different levels with their spatial distances from center of blasting source being almost identical were processed and analyzed. Three testers were respectively located and arranged at haulage-level roadway baseboard (Fig. 11a), 3-1road-connecting baseboard at No.3 hierarchy (higher than haulage-level roadway by about 10m, Fig. 11b) and 2-1road-connecting baseboard at No.2 hierarchy (higher than haulage-level roadway by about 20m, Fig. 11c) in the 16th level, and HHT analysis was conducted

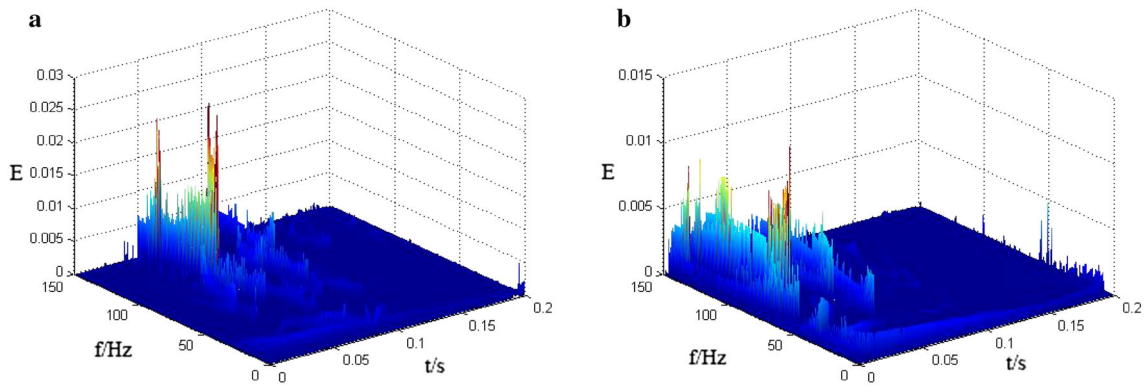


Fig. 10 3D spectrum

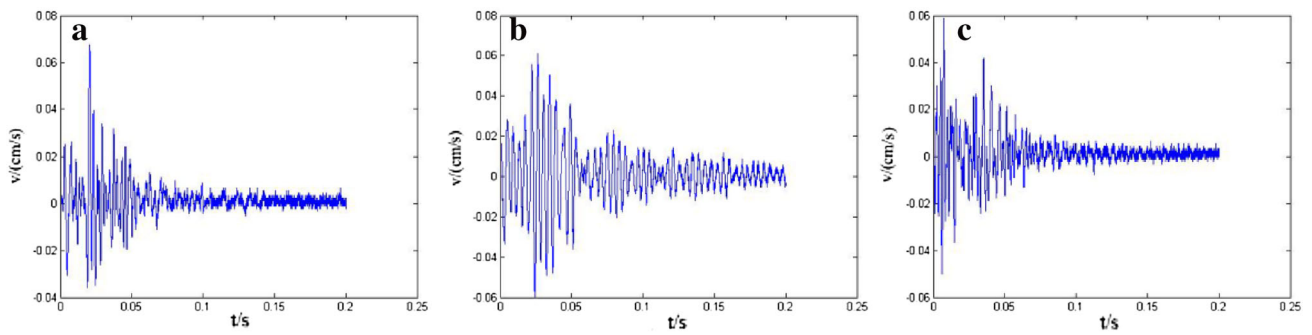


Fig. 11 Original oscillogram

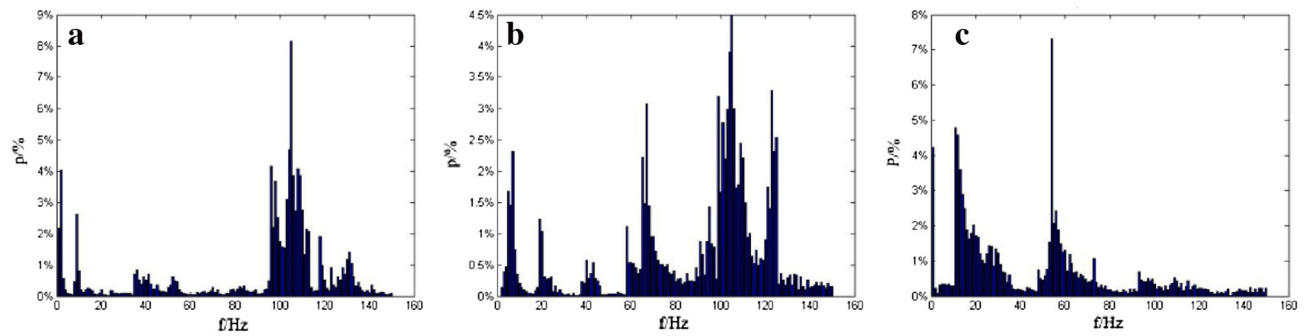


Fig. 12 Energy distribution

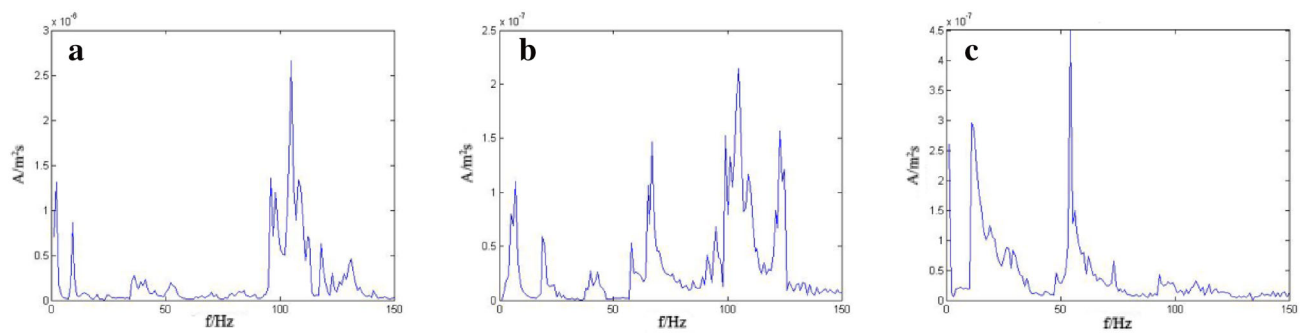


Fig. 13 Marginal spectrum

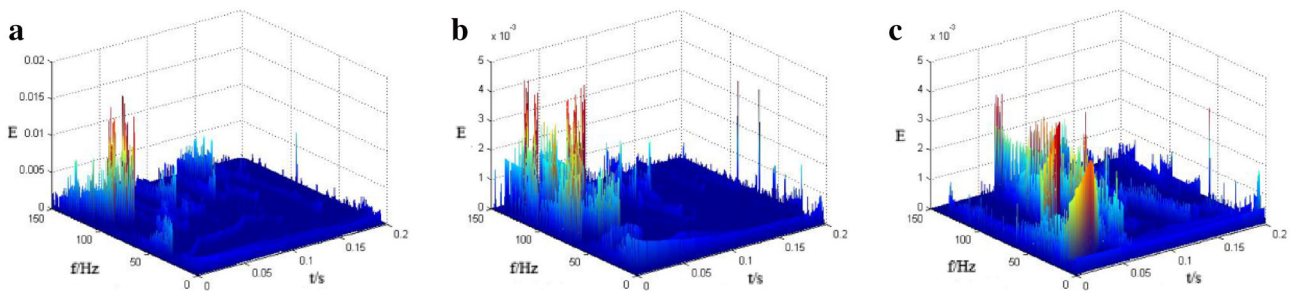


Fig. 14 3D spectrum

Table 6 The table of permissible standard for blasting vibration safety

Protection object categories	Safe allowable particle vibration velocity (cm/s)		
	$f \leq 10\text{ Hz}$	$10\text{ Hz} < f \leq 50\text{ Hz}$	$f > 50\text{ Hz}$
Mine workings	15–18	18–25	20–30

on them as below. Original oscillogram through transformation was as shown in Fig. 11.

It could be known from Table 3 that under the circumstance that maximum single blow blasting charge remained unchanged, as level where monitoring point was arranged continuously rose, in data collected by tester, peak vibration velocity of vertical component continuously reduced, and frequency also drew close to low frequency.

a, b and c in Fig. 12 was energy distribution diagram of respectively haulage-level roadway baseboard, 3-1 road-connecting baseboard at No.3 hierarchy and 2-1 road-connecting baseboard at No.2 hierarchy in the 16th level. In a, energy distribution of blasting signals concentrated at 95–140 Hz frequency band; in b, it could be obviously seen that energy distributed in a large quantity within 60–150 Hz, but compared with a and b, within 0–20 Hz frequency band, energy occupancy increased; in c, 10–35 and 50–75 Hz occupied a minority of energy distribution. It could be seen by comparing a, b and c that energy distribution of blasting vibration signals moved from high frequency band to low frequency band as hierarchy rose. Figure 13 was marginal spectrum of three hierarchies. In a, maximum amplitude appeared within 100–110 Hz, while amplitudes in other frequency bands were relatively not high; in b, maximum amplitude also appeared within 100–110 Hz, but within 100 Hz, amplitude occupancy prominently increased when compared with that in a; in c, maximum amplitude appeared within 50–60 Hz, amplitude within 10–35 Hz was greater than those in a and b. It could be seen by comparing a, b and c in Fig. 13 that amplitude also moved from high frequency band to low frequency band as hierarchy rose. It could be known through comprehensive and comparative analysis of 3D spectrum in Fig. 14 that: in vertical direction, with an increasing number of spanned underground systems, main vibration band of blasting vibration signals gradually devel-

oped towards middle and low frequencies, in the meantime, proportion of components of middle and low frequency signals in energy increased.

It could be known from permissible standard for blasting vibration safety (Table 6) in Safety Regulations for Blasting (GB6722-2014) [20] that: as natural vibration frequency of engineering structure like Shizishan copper mine was usually low, during propagation process of blasting seismic waves, although strength of blasting vibration continuously reduced, its damaging effect could possibly become more obvious. This requires the accurate monitoring and analysis of the frequency intensity of blasting vibration to prevent accidents.

6 Conclusion

1. To study propagation rule of blasting seismic wave signals of deep stope of Shizishan copper mine, this paper collected blasting seismic wave signals produced by blasting in the 16th level, make a regression analysis of collected blasting vibration velocity, and obtained values of coefficient and attenuation index K and related to landform and geological conditions from blasting point to monitoring point in Shizishan copper mine as well as corresponding blasting vibration propagation formula.
2. According to permissible distance standard for safety of blasting vibration in Safety Regulations for Blasting (GB6722-2014) [20], it took maximum vibration velocity of vertical component of on-site blasting vibration as 15 cm/s, combined Sadov’s linear regression formula obtained through fitting and considered safety production, it selected calculation result of formula $V = 281.2(\frac{\sqrt[3]{Q}}{R})^{1.535}$ to determine maximum single blow blasting charge for safe detonation so as to guide actual production blasting on the site.

3. HHT analytical method was used to analyze propagation rule of seismic waves produced by two different monitoring schemes, and it is found that: as maximum tolerant explosive quantity of single shot increased and number of spanned underground systems increased, energy of blasting vibration signals reduced at high frequency band, energy distribution at middle and low frequency bands increased, especially it increased obviously within 0–20 Hz frequency band.
4. Combining Sadov's linear regression formula and results obtained from analysis with HHT algorithm, maximum single blow blasting charge should be controlled, and frequency of blasting vibration signals should be controlled within high frequency band so as to ensure safety production in the mine.

Acknowledgements This work was supported by National Natural Science Foundation of China, Grant Numbers 51564027, 41362013. This paper is also supported by the opening project of State Key Laboratory of Explosion Science and Technology (Beijing Institute of Technology). The opening project number is KFJJ15-14M.

References

1. Xiaoming, Y.E., Delun, W.U.: A comprehensive review and commendation of blastvibration safety velocity. *Chin. J. Rock Mech. Eng.* **16**(3), 266–273 (1997)
2. Zhixin, Y., Yong-he, W., Ping, J., et al.: Study on measurement of blast-induced seism and building safety criteria. *Chin. J. Rock Mech. Eng.* **22**(11), 1907–1911 (2003)
3. Xie, C., Luo, Z., Jia, N., et al.: Dynamic effects of open blasting vibration on adjacent buildings and measures for vibration reduction. *J. Vib. Shock* **32**(13), 187–193 (2013)
4. Ling, T., Li, X.: Influence of maximum decking charge on intensity of blasting vibration. *J. Cent. S. Univ.* **13**(3), 286–289 (2006)
5. Yang, R.L., Rocque, P., Katsabanis, P., et al.: Measurement and analysis of near-field blast vibration and damage. *Geotech. Geol. Eng.* **12**(3), 169–182 (1994)
6. Hongxian, F., Yong, Z., Jinshui, X., et al.: Study of blasting vibration test of area near tunnel blasting source. *Chin. J. Rock Mech. Eng.* **30**(2), 335–340 (2011)
7. Guangxi, Y., Haitao, Y., Liu, X., et al.: Test and analysis of an existing tunnel vibration induced by blasting construction of diaphragm wall. *Trans. Tianjin Univ.* **14**(1), 569–575 (2008)
8. Weiye, L.: Analysis of the Blasting Vibration in Tunnel Surrounding Rock and the Stability of Supporting Structure. Wuhan University Of Science and Technology, Wuhan (2012)
9. Li, X., Long, Y., Ji, C., et al.: Dynamic stress concentration factor for tunnel surrounding rock under blasting seismic waves. *Chin. J. Geotech. Eng.* **35**(3), 578–582 (2013)
10. Kahrman, A., Ozer, U., Aksoy, M., et al.: Environmental impacts of bench blasting at Hisarcik Boron open pit mine in Turkey. *Environ. Geol.* **50**(7), 1015–1023 (2006)
11. Yuanjuan, Z.: Inference of Blasting Vibration to Open-Pit Slope and Vibration Prediction. Wuhan University of Technology, Wuhan (2012)
12. Wang, J., Luan, L., Zhang, Z., et al.: Numerical simulation of blasting vibration effect on stability of high-steep slope. *Blasting* **29**(3), 119–122 (2012)
13. Ramulu, M.: Development of a new blast vibration prediction model incorporating burden variations in surface blasting. *Int. J. Geotech. Earthq. Eng.* **1**(2), 72–88 (2010)
14. Song, G.M., Shi, X.Z., Zhou, Z.G., et al.: Monitoring and assessing method for blasting vibration on open-pit slope in Hainan iron mine. *J. Cent. South Univ.* **7**(2), 72–74 (2000)
15. Junru, Z., Wenbo, L., Le, Z., et al.: Attenuation of vibration frequency during propagation of blasting seismic wave. *Chin. J. Rock Mech. Eng.* **33**(11), 2171–2178 (2014)
16. Zhenyang, X., Yang, J., Chen, Z., et al.: Blasting seismic waves energy distribution based on EEMD. *J. Vib. Shock* **33**(11), 38–42 (2014)
17. Zhong, G.S., Li-Ping, A.O., Zhao, K.: Influence of explosion parameters on wavelet packet frequency band energy distribution of blast vibration. *J. Cent. S. Univ.* **19**(9), 2674–2680 (2012)
18. Yan, W.M., Yuen, K.V.: On the proper estimation of the confidence interval for the design formula of blast-induced vibrations with site records. *Rock Mech. Rock Eng.* **48**(1), 361–374 (2015)
19. Yanhui, G.: Shizishan Copper Mine Deep Mining Rock Mass Caving Mining Technology and Surface Movement Law Research. Kunming University of Science and Technology, Kunming (2011)
20. Standards of the People's Republic of China (GB6722-2014): Safety Regulations for Blasting. China Standard Press, Beijing (2014)
21. Xibing, L., Desheng, G.: Rock Impact Dynamics. Central South University of Technology Press, Changsha (1994)
22. Zhao, W.: Rock Mechanics. Central South University Press, Changsha (2010)
23. Guozhong, H., Wang, H., Li, X., et al.: Research on blasting vibration regularity of bedrock digging of embankment project. *Rock Soil Mech.* **S2**, 1036–1040 (2006)
24. Huang, N.E., Shen, Z., Long, S.R., et al.: The empirical mode decomposition and the hilbert spectrum for nonlinear and non-stationary time series analysis. *Proc. R. Soc. Lond.* **1998**(454), 903–995 (1971)
25. Huang, N.E.: A new method for non-linear and non-stationary time series analysis: the Hilbert spectral analysis. *Proc. SPIE* **4056**, 197–209 (2000)
26. Xibing, L.: Analysis of Blast Vibration Signals-Theories and Methods. Science Press, Beijing (2009)
27. Xibing, L., Yiping, Z., Zhixiang, L., et al.: Wavelet analysis and Hilbert–Huang transform of blasting vibration signal. *Explos. Shock Waves* **25**(6), 528–535 (2005)
28. Li, X., Li, Z., Wang, E., et al.: Analysis of natural mineral earthquake and blast based on Hilbert–Huang transform (HHT). *J. Appl. Geophys.* **128**, 79–86 (2016)
29. Li, L., Wang, F., Shang, F., et al.: Energy spectrum analysis of blast waves based on an improved Hilbert–Huang transform. *Shock Waves* **2016**, 1–8 (2016)
30. Dong, Y., Li, Y., Xiao, M., et al.: Analysis of earthquake ground motions using an improved Hilbert–Huang transform. *Soil Dyn. Earthq. Eng.* **28**(1), 7–19 (2008)
31. Sun, Q., Wang, M., Yushan, X., et al.: HHT analysis and application of blasting vibration in rock roadway excavation. *Eng. Blast.* **1**, 1–7 (2016)



Xianglong Li received the Ph.D. degree in geotechnical engineering from China University of Mining and Technology-Beijing (CUMTB), Beijing, P.R. China, in 2010. He is currently an associate Professor with the Faculty of Land Resource Engineering, Kunming University of Science and Technology (KUST). His current research interests include blasting engineering, geotechnical engineering and mining engineering.



Lihua He received the Master Degree in Engineering in safety engineering from Kunming University of Science and Technology (KMUST), Kunming, Yunnan, P.R. China, in 2007. She is currently a lecturer with Faculty of Mining Industry, Kunming Metallurgy College. Her current research interests include safety engineering and mining engineering.



Hui Hu received the Bachelor's Degree in safety engineering from Henan Institute of Engineering, Zhengzhou, Henan, P.R. China, in 2015. He is currently studying for a master's degree at Kunming University of Science and Technology (KUST), Kunming, Yunnan, P.R. China. His current research interests include mining technology, blasting engineering and safety engineering.



Kegang Li received the Ph.D. degree in mining engineering from Chongqing University (CQU), Chongqing, P.R. China, in 2006. He is currently a Professor with the Faculty of Land Resource Engineering, Kunming University of Science and Technology (KUST). His current research interests include rock mechanics, stability of underground engineering and slope engineering.